Design and Testing of a Submersible Laboratory-Sized Cryogenic Liquid Hydrogen Pump

H Bischoff*, J Doll, C Haberstroh and C. Thomas

Schaufler Chair of Refrigeration, Cryogenics and Compressor Technology,
TUD Dresden University of Technology, Dresden, Germany

*E-mail: henrik-gerd.bischoff@tu-dresden.de

Abstract. As the hydrogen market expands, the need for the efficient distribution of liquid hydrogen (LH_2) becomes increasingly important. Reducing flash gas losses during LH_2 transfer and ensuring adequate pressurization of downstream applications, such as fuel cells and combustion engines, are challenges. It is therefore essential to develop pumps for liquid hydrogen. To overcome transfer losses a three-staged liquid hydrogen turbo pump, as well as a test rig for small cryogenic pumps was developed. This paper presents the general concept of this submersible liquid hydrogen pump and gives insight into component and system testing of this pump.

1. Introduction

As the hydrogen market continues to grow, the efficient distribution of liquid hydrogen (LH_2) becomes increasingly critical. Key challenges include minimizing flash gas losses during LH_2 transfer and ensuring sufficient pressurization for downstream applications such as fuel cells and combustion engines. To address these challenges, it is essential to develop liquid hydrogen pumps of various sizes, optimized for different flow and pressure requirements. The objective of this project is to design and develop a laboratory-scale liquid hydrogen turbopump specifically for transfer applications.

This paper presents basic thermodynamic considerations of LH_2 transfer, the general concept of the developed submersible turbopump, highlights key mechanical design decisions, describes the associated test rig for small cryogenic pumps and provides initial testing insights.

2. Thermodynamics of LH_2 transfer

The transfer of LH_2 poses unique thermodynamic challenges. Since H_2 has a normal boiling point of 20.28 K, any heat ingress into the liquid leads to continuous boiling during storage. As a result, cavitation – the formation and possible collapse of vapor bubbles caused by local pressure dropping below saturation pressure – can occur especially at the impeller inlet of a pump. To reduce the risk of cavitation, an inducer can be used for pre-pressurization of the first pump stage.

In addition to cavitation, flash gas generation is a loss mode of LH_2 transfer. Most LH_2 transfer applications rely on differential pressure to transfer the liquid from one dewar to another dewar. This is performed by connecting the dewars. The starting dewar is equipped with a riser line and gets pressurized. If the pressurizing occurs slowly saturated fluid can be assumed; if the pressurization is done quickly, subcooled fluid can be assumed. The receiving dewar is at a lower

Content from this work may be used under the terms of the Creative Commons Attribution 4.0 licence. Any further distribution of this work must maintain attribution to the author(s) and the title of the work, journal citation and DOI.
Published under licence by IOP Publishing Ltd

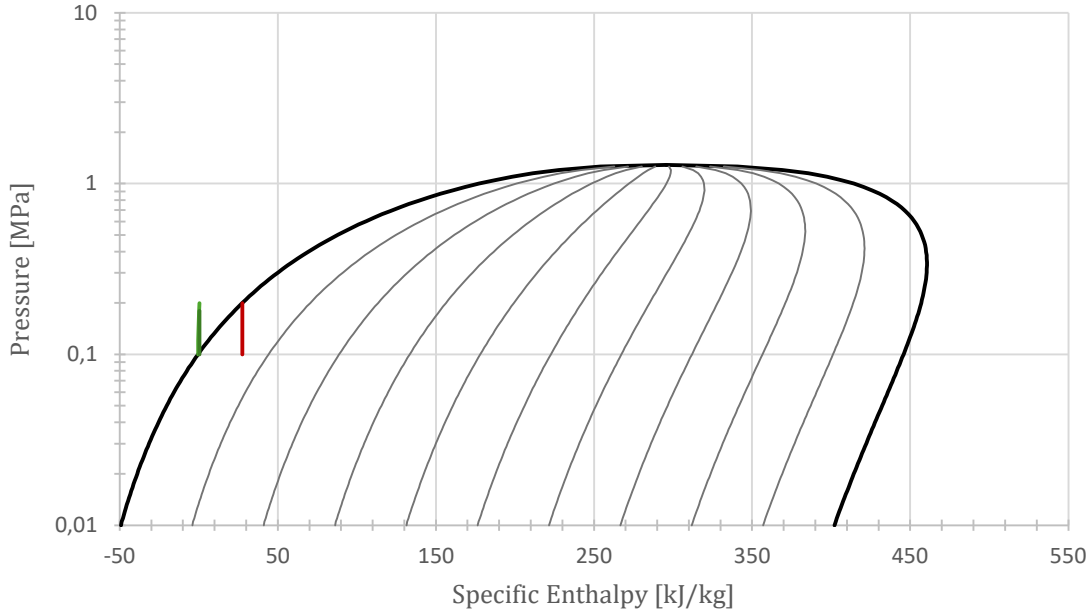

Figure 1 *log* p, h – diagram of para hydrogen; expansion while transfer by pressure difference 2 bar_a to 1 bar_a(red); transfer process by pump (green)

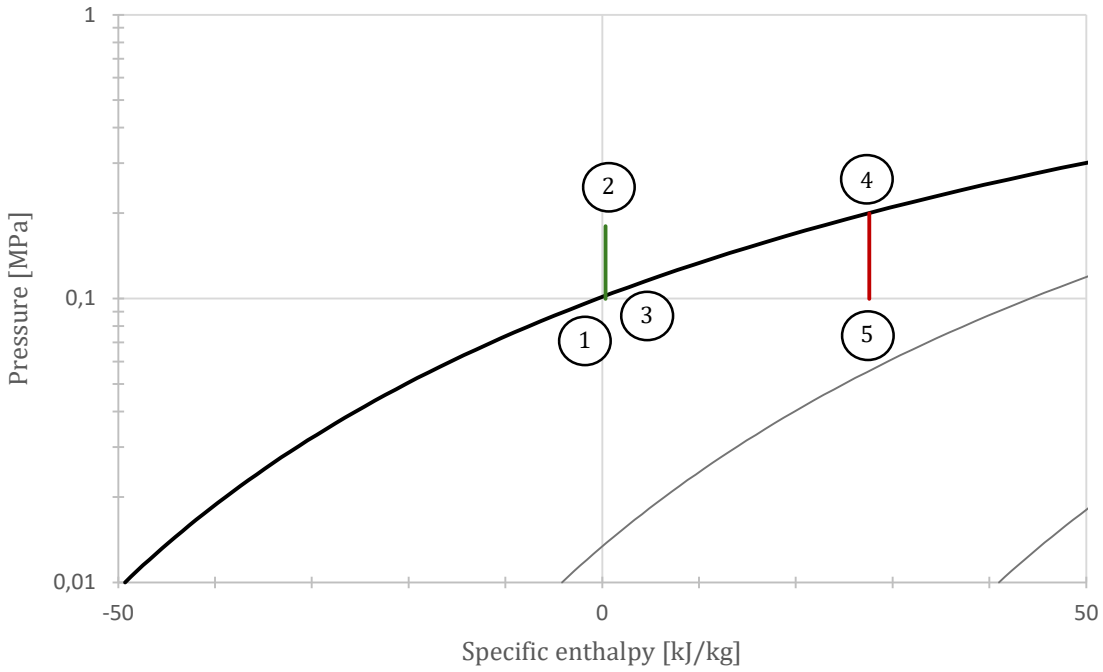

Figure 2 Crop of *log* p, h – diagram of para hydrogen; expansion while transfer by pressure difference 2 bar_a to 1 bar_a(red); transfer process by pump (green)

pressure level than the starting dewar. Liquid gets transferred. The pressure drop over the line can thermodynamically be described as isenthalpic expansion, which can lead to partial vaporization. In contrast, a pump enables isentropic compression, resulting in subcooled liquid at the pump outlet. This subcooling creates an enthalpy buffer, which significantly reduces flash gas formation during expansion. *Figure 1* illustrates a logarithmic pressure-enthalpy (log p-h) diagram of parahydrogen.

The red and green lines show the ideal, isenthalpic transfer processes. The green lines pressurizing and expansion processes using a pump. The red line shows the expansion of transfer by differential pressure. *Figure 2* shows a crop of *Figure 1* to put an emphasis to the processes. The transfer by pump starts at approximately ambient pressure, saturated liquid (1). The pump pressurizes the fluid with an approximated efficiency $\eta_{is} = 47.5\,\%$ to 2 bar_a (2), which was determined by considering empirical correlations. The subcooled fluid gets expanded to ambient pressure. The expansion process reaches into the two-phase region, thus ~ 0.2 % flash gas gets generated (3). The transfer by differential pressure is described as isenthalpic expansion from 2 $bara$ saturated fluid (4) into the two-phase region (5). Hereby ~ 6 % of the LH_2 evaporate.

Thermodynamically, the use of a pump can accelerate the liquid transfer process and minimize flash gas loss, making it a favourable option for efficient LH_2 handling.

3. Mechanical design of the LH2 pump

The chosen design point of the LH_2 pump is $\dot{V} = 2100\frac{\mathrm{l}}{\mathrm{h}}$ at a pressure difference of $\Delta p = 1$ bar between the suction and the discharge port. The pump should be as small as possible, feature a modular design and be submergible.

First design was made according to the Blaha and Balje chart for pumps. Figure 3 (left) shows the Blaha chart, which helps to choose the right pump type for a given application. With the given design(point) the specific work Y can be calculated with *Eq. 1*. The specific speed is calculated by the volume flow $\dot{V}$ and the rotational speed n, see *Eq. 2*. With a rotational speed of $n = 16000$ rpm a turbo pump is suited for the transfer application.

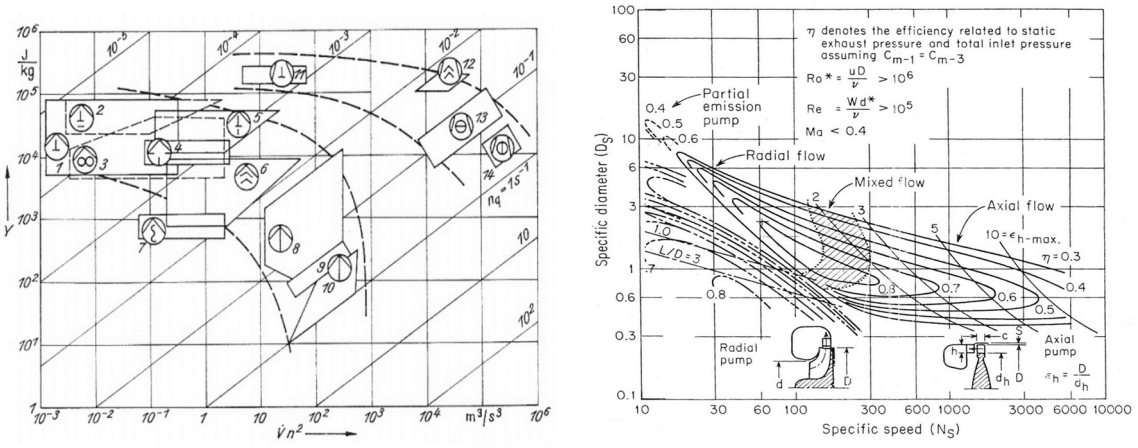

Figure 3 Blaha chart (left) [1]; Balje chart / Ns-Ds-chart (right) [2]

$$Y = \frac{\Delta p}{\rho} = \frac{1 \cdot 10^5 \text{Pa}}{70.88 \frac{\text{kJ}}{\text{kg}}} = 1.41 \cdot 10^3 \frac{\text{J}}{\text{kg}} \tag{1}$$

$$\dot{V} \cdot n^2 = 5.83 \cdot 10^{-4} \frac{\text{m}^3}{\text{s}} \cdot \left(266.7 \frac{1}{s}\right)^2 = 41.48 \frac{m^3}{s^3} \tag{2}$$

On the right-hand side of *Figure 3* the N_S-D_S-chart is shown. With a specific diameter and a specific speed Ns, see *Eq. 3* (not the same as in the Balje chart) and a specific diameter Ds, see *Eq. 4* the expected efficiency of a single stage can be derived. As *Eq. 4* shows the outer diameter of the impeller has an impact to the efficiency. This leads to an optimum for the size and number of the impeller.

Table 1. Efficiency vs. number of stages

Number of stages [-]	Specific Diameter [-]	Specific Speed [-]	Diameter [mm]	Stage Efficiency [%]
1	6.4	22.6	60	45
2	3.4	38.1	43.5	65
3	2.6	51.7	32.5	78

$$N_S = \left[\frac{N}{\text{rpm}}\right] \cdot \left[\frac{\dot{V}}{\frac{\text{ft}^3}{\text{s}}}\right]^{\frac{1}{2}} \cdot \left[\frac{H}{\text{ft}}\right]^{-\frac{3}{4}} \tag{3}$$

$$D_S = \left[\frac{D}{\text{ft}}\right] \cdot \left[\frac{H}{\text{ft}}\right]^{\frac{1}{4}} \cdot \left[\frac{\dot{V}}{\frac{\text{ft}^3}{\text{s}}}\right]^{-\frac{1}{2}} \tag{4}$$

Tab. 1 shows the number of stages and the efficiency per stage. With three stages not only a good efficiency, but also a compact size can be accomplished. The hydraulic design of the inducer, impeller and stators was done in CFturbo. The pump is designed as a three-stage radial full emission turbo pump. Figure 4 (left) shows a sectional view of the pump, with the fluid path. The main components are shown. The fluid path begins at the suction side. The first rotating part is the inducer. This axial section has a lower work transmission compared to the impellers and provides sufficient pre-pressurization for the first impeller. This reduces the risk of cavitation at the suction side. The inducer and the 1st impeller are designed in one piece. After the 1st impeller the fluid is diverted 180° and fed into a stator. It converts kinetic energy into pressure and prepares the flow for the following stage. A compact back-to-back design is chosen to keep the outer diameter of the pump small. The first stage is followed by a similar impeller stator arrangement. The 3rd stage has the same impeller, but the stator design is different. The fluid flow gets directed around the motor. On the top of the motor is the discharge port located. The inducer and impellers are mounted on a shaft. Since the stators between the impellers do not rotate, spacers are used to set the distance between the rotating parts on the shaft. The shaft features a shoulder on the upper side. At the lower side a screw axially braces the components. The torque is transmitted frictionally from the shaft to the rotating components. The not rotating stators are

positioned by centering rings. The centering rings have two purposes; first, they centre the stators and position them relative to each other, secondly, they act as sealing due to their tight fit. The sealing between the stages is done by a single sided labyrinth gap sealings. To make the sealing work, the gaps need to be small. The radial gaps are 0.2 mm wide. Axial gaps range from 0.2 mm to 1 mm to accommodate for tolerance stacking. Small gaps are chosen for the higher-pressure side and wider tolerances on the lower pressure side. The pump is made of austenitic steel (1.4404 / AISI 316L eq.). Austenitic steel is not only cold-tough, but also resistant to hydrogen embrittlement [3]. Most parts are designed to be conventionally manufactured, except the inducer, impeller and the stators. Those parts are metal 3D printed using metal-binder-jetting process and machined afterwards.

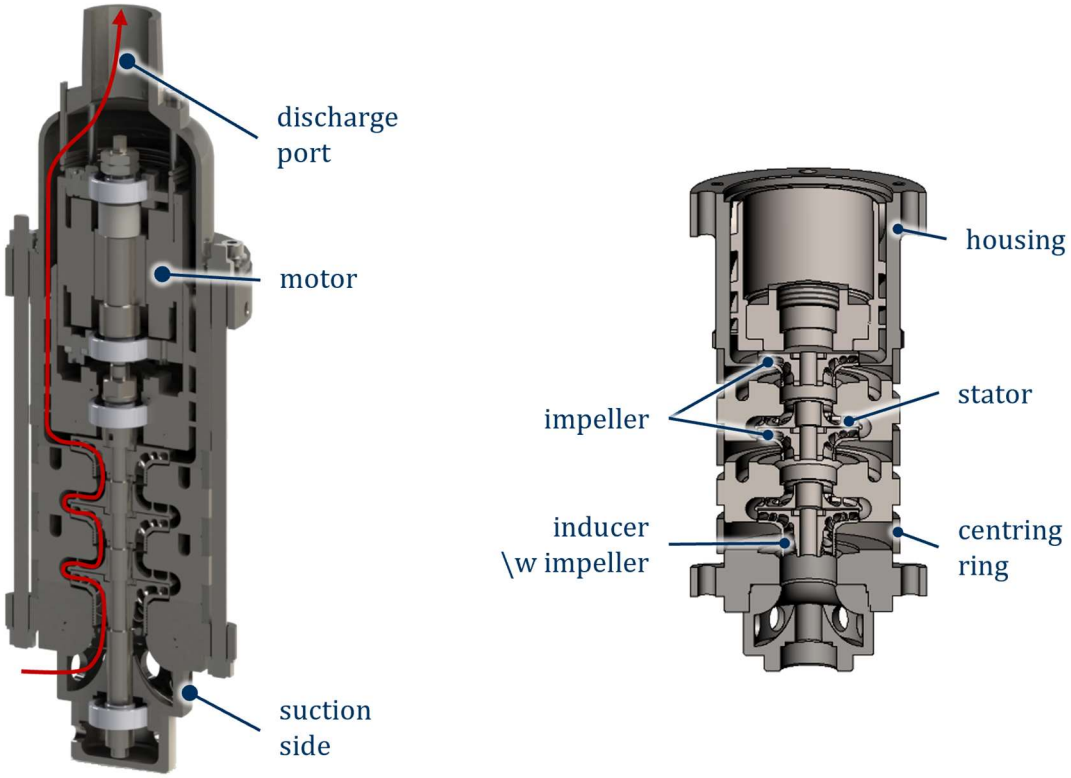

Figure 4 Sectional view of the LH_2 pump (left); explosion view of the pump side (right)

On top of the output drive the motor is located. First, it was anticipated to use a brushless direct current (BLDC)-motor. The rotor of this BLDC motor integrates a permanent magnet. Usually NdFeB magnets are used, because of their high magnetic field density. NdFeB and SmCo magnets were tested regarding their hydrogen compatibility. NdFeB was being exposed to gaseous hydrogen at 10 bar at ambient temperature for 7 days. The NdFeB-Magnet disintegrated. Thus, an induction motor was chosen to drive the LH_2 pump. The motor is built on a purpose made rotor and stator combination built by “e+a Elektromotoren AG”. It is called “DBL 120623” and designed to work submerged in LH_2.

Figure 5 shows a cross sectional view of the self-designed motor. The stator is press fit into the housing of the motor. The rotor sits on the motor shaft. An Invar spacer is used to keep the distance to the fixed bearing. The bearing itself is fixed on the shaft by two nuts. The Invar spacer

has a lower thermal contraction than stainless steel [3]. So a frictional connection between the rotor and the shaft works even better at low temperatures. The end shield on the upper side of the motor is welded to the housing. On top of the upper end shield there is a cover that fixates the upper bearing. The end shield on the lower side is screwed in. It provides the guide for the floating bearing. The floating bearing is axially positioned by a thin sheet metal spring.

To bear the motors and the pumps shaft special made cryogenic hybrid bearings, of the size DIN625 626, were bought. The bearing races are made of martensitic steel (1.4125) with a tungsten disulphide coating. The ceramic balls are made of a silicon nitride (Si_3N_4-YA1). The cage is made of an unspecified black PTFE mixture.

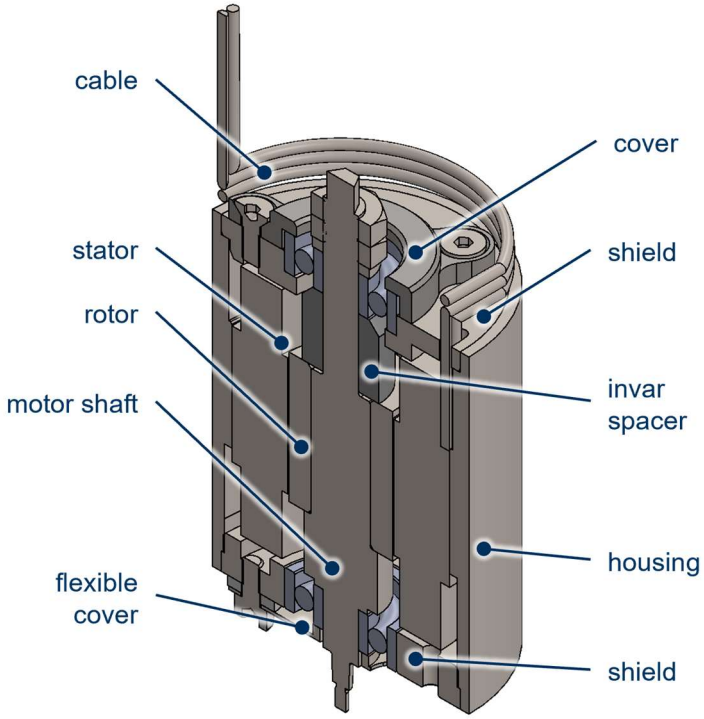

Figure 5 motor for LH_2 pump, 90W, 16 000 rpm

4. First Tests

The first tests were conducted at room temperature to check whether the rotor system is grinding. The motor itself and the motor within the pump could reach their working speed of 16000 rpm without major problems. Only a few minor mechanical touch-ups needed to be done. There is no need to balance the rotating parts, since the minor resonance does not have an impact to the function of the assembly.

After the room temperature tests, tests within liquid nitrogen (LN_2) were performed. Experiments in LN_2 can be conducted in a safe and easy way at the cryogenic laboratories of Dresden University of technology (TUD). To reduce the mechanical complexity, motor and pump were tested separately. It allows to identify possible problems easier. The motor test in LN_2 was performed by putting the motor into a see-through cryostat. The cryostat was three times evacuated to 10^{-3} $mbar$ and purged with nitrogen (pump and purge). This ensures little to no

residual gases that may freeze out and block the bearings. After the pump and purge cycles the motor slowly operated at 200 rpm during filling with liquid nitrogen. When the motor was fully submerged it was turned off. Different speed ramps up to 16000 rpm were driven.

The next step is to verify that the pump set up runs in LN_2. The pump was mounted inside the same cryostat, similar pump and purge cycles were performed. The cooldown was also performed with the pump slowly spinning. After the fill level has completely passed the 1st stage of the pump, the LN_2 supply was switched off. Since the pump was still spinning, the speed was slowly raised to 7000 rpm. LN_2 was successfully pumped. After 15 min of operation the pump started to sound differently. Shortly afterwards the rotation stopped with a screeching sound. The experiment was ended. After warming up the assembly the pump could be started again. It is assumed, that the rotor became too warm. The heat may get transferred through the shaft to the bearings. The inner ring of the bearings may have heated up and expanded. This may explain the blockage. Further investigation is needed.

In future, further tests within liquid helium (LHe) and liquid hydrogen (LH_2) are planned. Therefore, a circulation testbench was build.

5. Testbench for cryogenic pumps

The built testbench for cryogenic pumps is designed as a circulating system. The pump draws the liquid from a reservoir. A valve provides hydraulic resistance to build up pressure.

Figure **6** shows the CAD of the testbench (left) and the picture of the manufactured testbench (right). All components can be seen. The pressure, temperature and volumetric flow can be measured. The pump pressure head is measured by a differential pressure transmitter (Keller, PD-33x ($\pm$ 0.5 mbar)) which is connected to the discharge pipe by a capillary tube. The temperature is measured by a SI diode by Lakeshore, which is into the discharge flow. The flow rate can be determined by a cryogenic flow meter using a cold turbine with magnetic pick-up coil (Hoffer Flow Controls, HO3/4x5/8 [3.4… 76 l/min]).

The measuring equipment enables the testbench to measure the thermodynamic state of the fluid behind the pump and the pumps performance.

6. Conclusion and Outlook

A pump for cryogenic fluids has the potential to reduce flash-gas losses and speeds up the transfer of cryogenic liquid. Building on this knowledge, a turbopump was designed and built. While designing the pump, an induction motor for cryogenic environments was engineered and built, too. Parallel to the development of the pump a testbench for cryogenic pumps was build.

First tests at room temperature and at LN_2 temperatures were mostly successful performed. Issues with the bearings were found, but the reason is unknown.

Further investigations with regard to the blocking bearings are necessary. After solving this problem, the pump will get characterized in LHe and LH_2 with the built testbench.

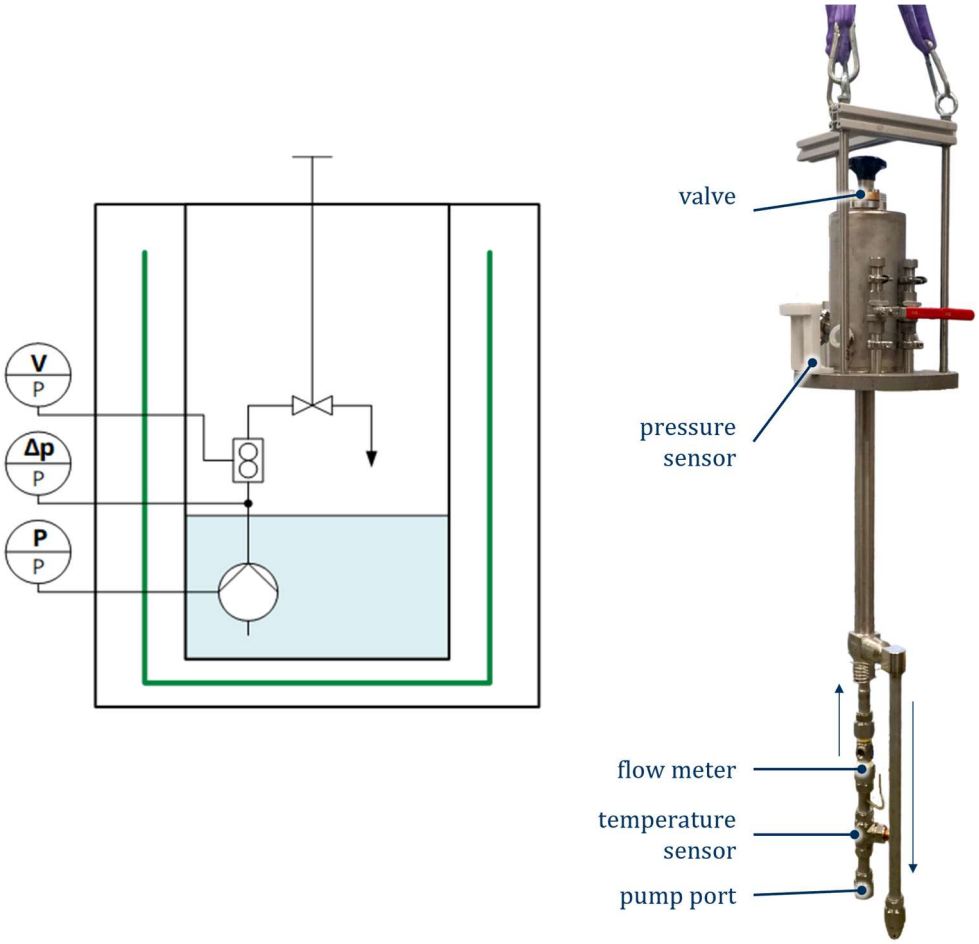

Figure 6 P&I diagram of the pump testbench(left); picture of the pump testbench (right)

Acknowledgements

This work was funded by the Federal Ministry of Education and Research (BMBF) under the 'TransHyDE' program (Project number: 03HY204B).

References

[1] Eifler W and Küttner K-H 2009 Küttner Kolbenmaschinen: Kolbenpumpen, Kolbenverdichter, Brennkraftmaschinen (Vieweg + Teubner)

[2] Balje O E 1962 A Study on Design Criteria and Matching of Turbomachines: Part B—Compressor and Pump Performance and Matching of Turbocomponents J. Eng. Power 84 1 https://doi.org/10.1115/1.3673350

[3] Ekin J W 2006 Experimental Techniques for Low-Temperature Measurements (Oxford: Oxford University Press) https://doi.org/10.1093/acprof:oso/9780198570547.001.0001